

On generation of Crab giant pulses

Maxim Lyutikov

Department of Physics, Purdue University,
525 Northwestern Avenue, West Lafayette, IN 47907-2036

October 26, 2018

Abstract

We propose that Crab giant pulses are generated on closed magnetic field lines near the light cylinder via anomalous cyclotron resonance on the ordinary mode. Waves are generated in a set of fine, unequally spaced, narrow emission bands at frequencies much lower than a local cyclotron frequency. Location of emission bands is fitted to spectral structures seen by Eilek *et al.* (2006).

To reproduce the data, the required density of plasma in the giant pulses emission region is much higher, by a factor $\sim 3 \times 10^5$, than the minimal Goldreich-Julian density. Emission is generated by a population of highly energetic particles with radiation-limited Lorentz factors $\gamma \sim 7 \times 10^7$, produced during occasional reconnection close to the Y point, where the last closed field lines approach the light cylinder.

Key words: plasmas - radiative transfer - waves - pulsars: Crab

1 Introduction

Giant pulses (GPs) are relatively rare durations of intense radio outbursts that are clearly a special form of pulsar radio emission (*e.g.* Kuzmin, 2007). Overall, the properties of GPs are (i) peak fluxes densities can exceed thousands (and, in case of Crab, nearly a million) of times the peak flux density of regular pulses (the Crab pulsar was discovered by observations of its giant pulses (Staelin & Reifenstein, 1968)); on average, energy coming in GPs can *exceed* the energy in an average pulse. Distribution of peak fluxes is power-law (unlike regular radio pulses which have Gaussian distribution); (ii) GPs typically have short duration from several microseconds down to few nanoseconds (Hankins et al., 2003) (much shorter than sub-pulses in the average pulse) and emit narrowband radiation (Popov & Stappers, 2003); at lower time resolution, overlap of many narrowband emission spectra may mimic a broadband spectrum; (iii) GPs seem to be limited to the edges of main profiles (*e.g.* Popov et al., 2006) (see, though, unconfirmed observations of GP in HFCs by Jessner et al. (2005)); (iv) GPs are seen in only 11 pulsars; (v) there is no correlation between GPs and emission

at higher frequencies (nothing in X-rays (Lundgren et al., 1995) and a marginal 3% correlation in the optical (Shearer et al., 2003)); (vi) there seems to be no strong correlation between pulsar properties (period, magnetic field, magnetic field at the light cylinder, luminosity) and GP phenomenon.

In addition, recent observation of Crab pulsar (Eilek & Hankins, 2007) identified unique features of GPs associated with the interpulse (IGPs): (i) IGPs spectra consist of a number of relatively narrow frequency bands; (ii) spacing between the bands is proportional, $\Delta\nu/\nu \sim 0.06$; (iii) emission at different bands start nearly simultaneous, perhaps with a small delay at lower frequencies; (iv) sometimes there is a slight drift up in frequencies; all bands drift together, keeping the separation nearly constant; (v) emission bands are located at 4–10 GHz, continuing, perhaps, to higher frequencies, but *not* to lower frequencies; (vi) all IGPs show band structure. These are very specific properties that allowed us to build a *quantitative* model of pulsar radio emission (applicable, at least, for Crab GPs associated with interpulse).

Theoretically, GPs were proposed to be nonlinear solitons (Mikhailovskii et al., 1985). Petrova (2004) proposed generation by induced scattering of waves leading to a redistribution of the radio emission in frequency. Weatherall (2001); Hankins et al. (2003) proposed strong plasma turbulence; Eilek & Hankins (2007) discuss a possibility of interference fringes. In spirit, our work is closest to Istomin (2004), who proposed that GP are generated on Alfvén waves during a reconnection event close to the light cylinder. On the other hand, discovery of the banded structure of IGPs is inconsistent with emission on Alfvén waves (see Appendix A), and, in addition, Alfvén cannot leave magnetosphere and need to be converted into escaping modes.

Before laying out the details we give here a brief overview of the model, Fig. 1. The model requires that a high density plasma, with density $\sim 10^5$ times Goldreich-Julian density, is present on closed field lines. In addition, an occasional high energy beam, with radiation-limited Lorentz factor $\sim 10^7$, is propagating along the field. These requirements come from actual fitting of observed emission bands to a particular cyclotron resonance conditions. The fit requires that the bulk plasma be not moving relativistically (hence association with closed field lines), the value of magnetic field be the minimum possible in the magnetosphere (even the factor of two difference of magnetic field strength between the magnetic pole and equator are important), emission region be limited to small volume (hence association with the Y-point).

2 Wave dispersion in pulsar magnetosphere

To guide the reader through the following derivations, we first re-derive the basic properties of wave dispersion in pair plasma in a strong magnetic field of pulsar magnetosphere. In the standard model of pulsar magnetospheres (Goldreich & Julian, 1969) rotating, strongly magnetized neutron stars induce strong electric fields that pull the charges from their surfaces. Inside the closed field lines of the neutron star magnetosphere, a steady charge distribution is established,

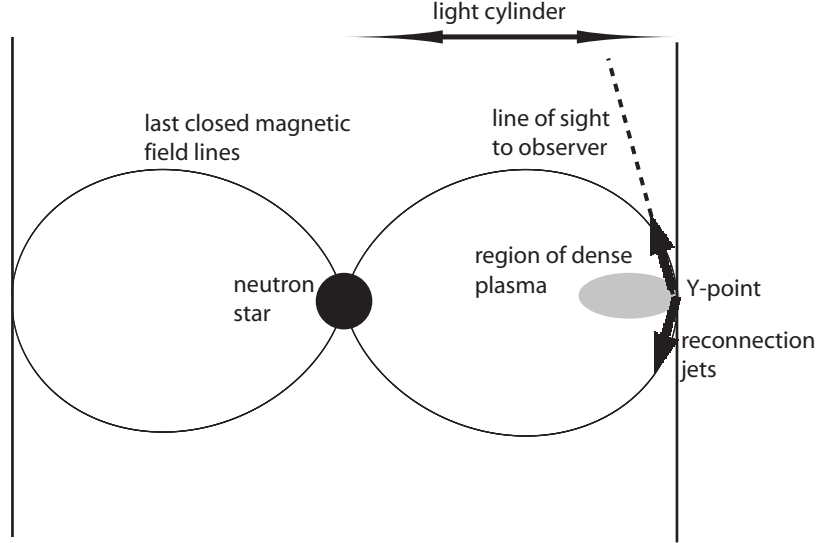


Figure 1: Generation region of giant pulses in Crab. High density plasma is trapped on closed field lines near the light cylinder. Occasional reconnection jets produce high Lorentz factor beams that propagate along magnetic field lines and emit coherent cyclotron-Cherenkov radiation at anomalous Doppler resonance.

compensating the induced electric field. It is typically assumed that on closed field lines, particle density is at a minimum and equals charge density, the Goldreich-Julian density $n_{GJ} = \Omega B / (2\pi c e)$. In fact, the real particle density may and does exceed this minimum value, as we argue in this paper. There is already a clear evidence that in case of the double pulsar PSR J0737–3039 plasma density on closed field line exceeds the Goldreich-Julian density by a factor $\sim 10^4 - 10^5$ (Lyutikov & Thompson, 2005), though it was not clear if this is specific to the double pulsar. One of the implications of the present model is that high density plasma is present on closed field lines of isolated pulsars as well.

As a simple parametrization, we normalize the plasma density to the Goldreich-Julian density, $n_p = \lambda n_{GJ}$. (We neglect the thermal motion of plasma particles and drifts resulting from curvature of field lines and inhomogeneity of magnetic field). The surface polar magnetic field of Crab pulsar is 3.7×10^{12} G. Below we will argue that *Crab GPs are generated near a magnetic equator*, where magnetic field at a given radius is two times smaller. Since the resonant frequency is proportional nearly to the third power of the local magnetic field (8), this factor of 2 is important. Thus, near the light cylinder the cyclotron frequency at the

equator is

$$\omega_B = \frac{9.5 \times 10^{12}}{(r/R_{LC})^3} \text{rads}^{-1} \quad (1)$$

For the density parameter $\lambda = 3.3 \times 10^5$ (see below), the corresponding plasma frequency is

$$\omega_p = \sqrt{2\lambda\Omega\omega_B} = \frac{3.4 \times 10^{10}}{(r/R_{LC})^{3/2}} \text{rads}^{-1} \quad (2)$$

($\nu_p = \omega_p/(2\pi) = 5.5 \times 10^9$ Hz). Thus, near the light cylinder $\omega_p/\omega_B \sim 2 \times 10^{-3}$ (this is the maximum value of this parameter as a function of r).

For e^\pm plasma in magnetic field the dispersion relation factorizes giving two modes: the X mode with the electric vector perpendicular to the $\mathbf{k}\text{-}\mathbf{B}$ plane and two branches of the longitudinal-transverse mode, which we will call L-O and Alfvén waves, with the electric vector in the $\mathbf{k}\text{-}\mathbf{B}$ plane (Arons & Barnard, 1986, see Fig. 2). X waves is a *subluminal* transverse electromagnetic wave with a dispersion relation

$$n^2 = 1 - \frac{2\omega_p^2}{\omega^2 - \omega_B^2} \quad (3)$$

here $n = kc/\omega$ is refractive index, $\omega_B = eB/mc$ is cyclotron frequency, $\omega_p = \sqrt{4\pi n_\pm e^2/m}$ is a plasma frequency of each species (so that for pair plasma the total plasma frequency is $\sqrt{2}\omega_p$). The Alfvén -L-O mode satisfies the dispersion relation

$$n^2 = \frac{(\omega^2 - 2\omega_p^2)(\omega^2 - 2\omega_p^2 - \omega_B^2)}{(\omega^2 - 2\omega_p^2)(\omega^2 - \omega_B^2) - 2\omega_B^2\omega_p^2 \sin^2 \theta} \quad (4)$$

Alfvén branch is always subluminal while L-O mode is *superluminal* at small wave vectors and *subluminal* at large wave vectors.

2.1 L-O mode

As we argue that the GPs are generated on the L-O mode, let us discuss its properties in more detail. The L-O mode exists in a frequency range

$$\sqrt{2}\omega_p < \omega < \left(\frac{1}{2} \left(\omega_B^2 + 2\omega_p^2 + \sqrt{(\omega_B^2 + 2\omega_p^2)^2 - 8\omega_B^2\omega_p^2 \cos^2 \theta} \right) \right)^{1/2} \approx \omega_B + \frac{\omega_p^2 \sin^2 \theta}{\omega_B} \quad (5)$$

It has a reflection point at $\sqrt{2}\omega_p$ and resonance at the upper bound. L-O mode becomes luminal at frequency $\omega_0 = \sqrt{2\omega_p^2 + \omega_B^2 \sin^2 \theta}$. Its polarization is

$$\frac{e_x}{e_z} = \frac{(\omega^2 - \omega_B^2)(\omega^2 - 2\omega_p^2) \cot \theta}{\omega^2(\omega^2 - \omega_B^2 - 2\omega_p^2)} \quad (6)$$

(for wave vector in $x - z$ plane), so that the L-O mode is nearly longitudinal for $kc \ll \omega_0$ (this becomes a Langmuir wave for parallel propagation) and is nearly transverse for $kc \gg \omega_0$. At the luminal point ω_0 polarization is quasi-longitudinal for $\theta \ll (\omega_p/\omega_B)^2$ and is quasi-transverse for larger angles.

3 Generation of giant pulses with banded frequency structure

3.1 Anomalous cyclotron resonance on L-O mode

The anomalous cyclotron resonance condition is

$$\omega - k_{\parallel} v_{\parallel} = s\omega_B/\gamma, \text{ for } s < 0 \quad (7)$$

where k_{\parallel} and v_{\parallel} are components of wave vector and particle's velocity along magnetic field, γ is Lorentz factor of fast particles and s is an integer. It is clear that the necessary requirement for the anomalous cyclotron resonance is that the refractive index of the mode be larger than unity, and that the parallel speed of the particle be larger than the wave's phase speed. The physics of emission is similar to the Cherenkov process, except that during photon emission a particle *increases* its gyration motion and goes *up* in Landau levels (Ginzburg, 1985). The energy is supplied by parallel motion. Importance of anomalous cyclotron resonance for pulsar radio emission has been discussed by Machabeli & Usov (1979); Kazbegi et al. (1991); Lyutikov et al. (1999). In these papers, emission was argued to be generated on open field lines at large distances from the start.

The resonant frequencies corresponding to anomalous cyclotron resonance for the X and L-O modes for our fiducial parameters (see below) are shown in Fig. 3. Overall, L-O mode dispersion is quite complicated, depending sensitively on the small parameters ω_p/ω_B and θ . As a guide we can use a much simpler condition for anomalous cyclotron resonance on X mode, keeping in mind that X mode has phase velocities larger than L-O mode. In the limit $\omega \ll \omega_B$ resonance on X mode occurs at frequencies

$$\omega \sim \frac{|s|\omega_B^3}{\gamma\omega_p^2} \quad (8)$$

Note, that for $\gamma \gg (\omega_B/\omega_p)^2$ both the resonant frequency and frequency differences are much smaller than cyclotron frequency. In case of relativistically streaming plasma on open field lines, the rhs of Eq. (8) is multiplied by γ_p^3 (where γ_p is Lorentz factor of plasma bulk motion), as plasma density, wave frequency and Lorentz factor are all smaller by $\sim \gamma_p$. As a result, for the fast, high field pulsar like Crab the resonance condition for radio waves cannot be satisfied inside the magnetosphere for reasonable plasma parameters. From (8) it follows that in order to have resonant frequency below ~ 10 GHz, it is required that $\gamma\lambda \geq 10^{13}$. This provides an order-of-magnitude estimate for the required plasma parameters. In making this estimate we neglected the Lorentz factor arising due to rotational velocities of emitting plasma, which can be important near the light cylinder.

Using the value of the magnetic field at the light cylinder (1) and parametrization of plasma density (2) we search through three parameters: plasma density normalization λ , Lorentz factor of the fast particles γ and viewing angle θ . To fit the results, we use Fig. 4 of Eilek & Hankins (2007), trying to reproduce

the frequencies and separations of the emission bands. We find a satisfying fit for the following parameters, see Fig. 4. Plasma over-density $\lambda = 3.3 \times 10^5$ (note, that this value is close to what was inferred for the plasma density on closed field lines of pulsar B in the double pulsar PSR J0737–3039 (Lyutikov & Thompson, 2005)). Lorentz factor of the fast beam is $\gamma = 7.4 \times 10^7$; this turns out to be close to the estimate of radiation-limited acceleration (10). The viewing angle with respect to magnetic field is $\theta = 0.0022$. A reasonable fit is achieved in a fairly limited volume of parameter space, $3.2 \times 10^5 < \lambda < 3.8 \times 10^5$, $6.9 \times 10^7 < \gamma < 7.4 \times 10^7$, $0.00251 < \theta < 0.00225$. Most importantly, for the first four bands the value of bands' separation $2(\nu_{s+1} - \nu_s)/(\nu_{s+1} + \nu_s)$ are .036, 0.053, 0.077, which is very close to the mean quoted value of 0.06.

3.2 Growth rates

Since for our best fit parameters $\theta \gg (\omega_p/\omega_B)^2$, Eq. (6) implies the L-O mode is nearly transverse at resonance. We can then use the previously calculated growth rates for excitation of transverse electromagnetic modes at anomalous cyclotron resonance (Kazbegi et al., 1991; Lyutikov et al., 1999)

$$\Gamma \sim \frac{\omega_{p,res}^2}{\omega} \quad (9)$$

where $\omega_{p,res}$ is the plasma frequency of the fast beam, generated during reconnection. Note, that since the emission bands' spacing is much smaller than their carrier frequencies, the growth rates are nearly the same for different bands (observed intensity also depends on saturation mechanism). Similar growth rate and, presumably, similar saturation levels explain generation of multiple emission bands. We expect that during a reconnection event, all the particles in the reconnection region may be accelerated, $\omega_{p,res} \sim \omega \sim \omega_p$, so that the Growth rate can be very high $\Gamma \sim \omega_p$

3.3 Lorentz factor of fast particles on closed lines

We envision that reconnection events close to the Y-point (near the last closed field lines at magnetic equator) accelerate particles along the closed field lines. The maximum available potential is related to the resistive process occurring during field reconnection, like the speed of reconnection and a number of flux tubes being reconnected. In addition, for nearly orthogonal rotators the "null charge surfaces" Cheng & Ruderman (1977), where Goldreich-Julian density vanishes, lies inside the polar cap, so that after reconnection a large potential drop would develop along the field lines Istomin (2004). The upper bound, which is not reached by far, can be estimated as the total potential across the open field lines, $\Phi \sim B_{NS} R_{NS} (\Omega R/c)^2$; this corresponds to a Lorentz factor $\gamma_{max} \sim 10^{11}$ (Istomin (2004) estimated Lorentz factor is about an order of magnitude smaller). The maximum electron energy will, in fact, be limited by radiative damping, like curvature and IC radiation. Assuming that curvature radiation is the dominant loss process, we can estimate the maximum energy than an electron can reach

in accelerating electric field $E \sim B$ (assuming that reconnection inflow velocity is close to the speed of light). We find

$$\gamma \sim \left(\frac{B}{e}\right)^{1/4} \sqrt{R_c} \sim 6.7 \times 10^7 \left(\frac{r}{R_{LC}}\right)^{-1/4} \quad (10)$$

where $R_c \sim c/\Omega$ is the curvature radius. Surprisingly, this matches nearly exactly the value that we inferred from fitting the observed narrow-band structure.

3.4 High plasma density on closed field lines

According to the model, a high density plasma should be present on closed field lines. The overdensity we find here, modeling Crab GPs, $\sim 10^5$, turns out to be close to the one found by eclipse modeling of the binary pulsar system PSR J0737-3039A/B Lyutikov & Thompson (2005). How related are these pieces of evidence and how dense plasma is created and supported on closed field lines? These two cases seem to be very different, in fact. In slow pulsars, like PSR J0737-3039B, plasma can be efficiently trapped on closed field lines by magnetic bottling (for $\sim 10^6$ periods in case of PSR J0737-3039B, Lyutikov & Thompson (2005)), but not in case of Crab, in which case radiative decay times are too short, $\sim 10^4$ sec at the light cylinder. Lyutikov & Thompson (2005) proposed that high densities on closed field lines of PSR J0737-3039B may be explained by interaction with the wind of the companion, but similar overdensity in an isolated pulsar questions that possibility. Though there are several ways particles can populate closed field lines (*e.g.* kinetic drift from open field lines, pair production by the 'backward' beam from outer gaps), the demands in case of short period pulsars like Crab are pretty high: the mechanism should create an over-density of the order 10^5 with no efficient bottling.

In case of Crab this over-density is required in a fairly limited region near the light cylinder, where IGPs are presumably produced. It is somewhat natural to associate this density enhancement with the Y-point, where the last closed field line approaches the magnetic equator. In fact, we indeed may expect high density around that region. First, even in rigidly rotating dipolar magnetosphere the charge density diverges at that point Goldreich & Julian (1969). Second, in case of a more realistic force-free aligned rotator, poloidal magnetic field also diverges at the Y-point Gruzinov (2005); Spitkovsky (2006). To resolve this divergency, non-ideal effects such as resistivity Spitkovsky (2006) and/or particle inertia Komissarov (2006) should be taken into account. At the moment, we leave this possibility to further studies.

3.5 Predictions: simultaneous GLAST signal

The model has interesting prediction for the forthcoming GLAST mission. The high energy beam is expected to produce curvature radiation at $\sim \hbar\gamma^3\Omega \sim 30$ GeV. This energy corresponds to the maximum effective area of the LAT instrument. Thus, one expects to see GeV photons contemporaneous with GPs.

Estimating the beam density $\sim n_{GJ}$ and emitting volume as $\sim 0.1R_{LC}^3$, the total power in curvature photons is $\sim 2 \times 10^{36}$ erg/sec, or 4×10^{37} photons/sec. Assuming isotropic emission (this gives a lower limit on the observed flux), the expected flux at Earth is $\sim 10^{-7}$ photons $\text{cm}^{-2} \text{s}^{-1}$ during a GP. This is nearly three orders of magnitude higher than the integral sensitivity of LAT at 30 GeV (for high latitude sources; Galactic background will also contribute in case of Crab), implying that a duty cycle of $\geq 10^{-3}$ for GP emission is needed to detect GP in GeV range. We conclude that we may reasonably expect GeV photons contemporaneous with GPs.

4 Implications of the model

Recent advances in observational technique uncovered very detailed properties of pulsar radio emission, and of Crab giant pulses in particular (Eilek & Hankins, 2007). Inspired by this work, in the present paper we describe a quantitative model of Crab giant pulses. To the best of our knowledge this is the first work on pulsar emission mechanism that actually does a fitting of pulsar spectra to a particular model. The model can reproduce fairly well the narrowband, unequally spaced emission bands seen in GHz frequency range in Crab giant pulses associated with the interpulse. It also explains why banded structure in IGPs in Crab is not seen below ~ 4 GHz: anomalous cyclotron resonance on L-O mode occurs above plasma frequency, which for our typical parameters is in the GHz range. Pulse to pulse variation in location of emission bands are due to fluctuations of the plasma density.

Note, that though the emission involves cyclotron transitions, both the emission frequencies and inter-band spacing are much smaller than the local cyclotron frequency for the best fit parameters. This is a curious property of anomalous cyclotron resonance.

Perhaps the most striking features of the model is that GPs are generated on *closed* field lines, in stark contrast to all other models of pulsar radio emission. We stress that this only applies to GPs, regular pulses are generated on open field lines, as is well established by a multitude of observational facts. We argue that giant pulses are different. The fact that we see GPs in some particular pulsars and that only the Crab IGP shows a banded frequency structure, is, in some sense, just a chance occurrence. The resonance condition is a sensitive function of the angle between the line of sight, local magnetic field and plasma density, so that a mismatch by $\sim 10^{-3}$ radians in observer angle either destroys the resonance completely or places the resonant frequency outside of the observed frequencies. This explains why GPs are typically seen in narrow phase windows. This may also be related to the fact that only few pulsars show GP phenomenon: in those cases we are lucky in terms of orientation, so that the line of sight passes close to the direction of local magnetic field at the reconnection region, and in terms of local plasma parameters, so that the emission frequency, which scales nearly $\propto \omega_B^3$ falls in the observed frequency range. Exact location of the reconnection region is not specified in the model, but it is naturally to assume

that it occurs close to the Y point, where we expect high current concentrations (Gruzinov, 2005).

One of the main implications of the model is that (at least near the Y-point) closed field lines are populated with dense plasma, exceeding by a factor 10^5 – 10^6 the minimum charge density. On the one hand, this is not expected from the basic pulsar model (Goldreich & Julian, 1969). On the other hand, presence of such dense plasma on closed field lines is solidly established in the case of the double pulsar PSR J0737–3039 (Lyutikov & Thompson, 2005). Somewhat surprisingly, the over-density $\sim 10^5$ (with respect to Goldreich-Julian density) we find here, modeling the generation of Crab giant pulsars, is similar to the over-density required to explain eclipses in the double pulsar.

To fit our findings into a global model of pulsar radio emission, we note that at frequencies above 2 GHz (but below NIR), Crab emission around the interpulse undergoes drastic changes with respect to both lower radio frequencies and higher optical through X-ray emission Moffett & Hankins (1996): the interpulse is shifted by ~ 10 degrees and new High Frequency Components (HFC1 and HFC2) trailing the interpulse appear. This is the range where the banded structure appears in IGPs. Our findings are consistent with the possibility that interpulse emission at these frequencies is a qualitatively different component from the main pulse and from the low frequency interpulse. Still a clear (geometrical?) picture of emission components is still missing.

For small angles of propagation with respect to magnetic fields, the dispersions of the X and the L-O modes nearly coincide, while polarization of both are nearly orthogonal for the parameters of interest. We have shown that the pattern of emission bands seen in IGPs matches well the anomalous cyclotron resonance on the L-O mode. On the other hand, resonance bands of the X mode may lie fairly close to the L-O modes, so it is natural to expect that the X mode should also be emitted. Emission bands associated with the X modes have distinctly different properties from L-O mode, being spaced in nearly equal intervals, equal to the frequency of the first harmonic. Large spacing, nearly the same as carrier frequency, makes it nearly impossible to observe X-mode emission bands with a finite receiver bandwidth (additional complications at low frequencies come from interstellar scattering). Still, the fact that a spectrum is not continuous, but consisting of emission bands, may be verified statistically during simultaneous observations of GPs in different frequency bands. Such observations of the millisecond pulsar B1937+21 (Popov & Stappers, 2003) showed that out of 10-15 GPs observed at two frequency windows 14141446 MHz and 22102250 MHz, no events were found to occur simultaneously at both frequencies. This requires that spectra of individual GPs are narrow band, $\Delta\nu/\nu \leq 0.5$, consistent with our picture.

Additional complications may come from absorption of the X-mode at cyclotron resonance. Since at the light cylinder the radiation frequency is much smaller than the local cyclotron frequency, resonant absorption may occur only in the wind (Sincell & Krolik, 1992). At distances much larger than the light cylinder, the radially propagating L-O mode is polarized nearly *along* magnetic field and thus is not absorbed at the cyclotron resonance (Petrova, 2006), while

the X mode may experience absorption.

The present model can also accommodate qualitatively the fact that sometimes emission bands seem to be drifting slightly up in frequency. If the fast beam is generated close to the magnetic equator, where magnetic field is the weakest, then as it propagates along the closed field lines, the local cyclotron frequency increases, leading to an increase of the observed frequency. Thus, placing beam generation region at magnetic equator explains why emission bands always drift up in frequency (Eilek & Hankins, priv. comm.).

At the moment it is not clear how rare or ubiquitous is the phenomenon of GPs in pulsars. As many as tens percent may show GPs (Ransom, priv. comm.). Of those pulsars that do show GPs, detection of banded structure in GPs depends sensitively on the plasma parameters close to the light cylinder and on the angle between line of sight and local magnetic field. Taking our best fit value of $\theta \sim 2 \times 10^{-3}$ we can estimate a relative number of pulsars in which we expect to see bands in GPs as $\sim \theta$. Such an estimate is very rough and is naturally subject to a number of uncertainties, like beaming fraction of normal and giant pulses.

Finally, we note that closed field lines of the Earth magnetosphere are very active in producing high brightness radio emission like auroral hiss, roars and burst (LaBelle & Treumann, 2002), though they all occur at normal cyclotron resonance (and thus require a loss cone-type distribution) at frequencies of the order of the local cyclotron frequency (and thus are too high to be directly applicable to observations of Crab pulsar at radio waves). It is intriguing to speculate that similar type emission might be observed from Crab at $\sim 10^{12} - 10^{13}$ Hz, but the required observations at such frequencies are challenging.

I would like to thank Timothy Hankins, Jean Eilek, Qinghuan Luo, George Machabeli, Alison Mansheim, Mikhail Popov and Scott Ransom for discussions that were vital for this work.

References

- Arons, J., & Barnard, J. J. 1986, *ApJ* , 302, 120
- Cheng, A. F., & Ruderman, M. A. 1977, *ApJ* , 216, 865
- Eilek, J. A., & Hankins, T. H. 2007, *ArXiv Astrophysics e-prints*
- Ginzburg, V. L. 1985, *Physics and astrophysics: A selection of key problems* (Oxford and New York, Pergamon Press, 1985, 139 p. Translation.)
- Goldreich, P., & Julian, W. H. 1969, *ApJ* , 157, 869
- Gruzinov, A. 2005, *Physical Review Letters*, 94, 021101
- Hankins, T. H., Kern, J. S., Weatherall, J. C., & Eilek, J. A. 2003, *Nature* , 422, 141

- Istomin, Y. N. 2004, in IAU Symposium, Vol. 218, Young Neutron Stars and Their Environments, ed. F. Camilo & B. M. Gaensler, 369–+
- Jessner, A., Słowikowska, A., Klein, B., Lesch, H., Jaroschek, C. H., Kanbach, G., & Hankins, T. H. 2005, *Advances in Space Research*, 35, 1166
- Kazbegi, A. Z., Machabeli, G. Z., Melikidze, G. I., & Smirnova, T. V. 1991, *Astrophysics*, 34, 234
- Komissarov, S. S. 2006, *MNRAS*, 367, 19
- Kuzmin, A. D. 2007, *ArXiv Astrophysics e-prints*
- LaBelle, J., & Treumann, R. A. 2002, *Space Science Reviews*, 101, 295
- Lundgren, S. C., Cordes, J. M., Ulmer, M., Matz, S. M., Lomatch, S., Foster, R. S., & Hankins, T. 1995, *ApJ*, 453, 433
- Lyutikov, M. 2000, *MNRAS*, 315, 31
- Lyutikov, M., Blandford, R. D., & Machabeli, G. 1999, *MNRAS*, 305, 338
- Lyutikov, M., & Thompson, C. 2005, *ApJ*, 634, 1223
- Machabeli, G. Z., & Usov, V. V. 1979, *Soviet Astronomy Letters*, 5, 238
- Mikhailovskii, A. B., Onishchenko, O. G., & Smolyakov, A. I. 1985, *Soviet Astronomy Letters*, 11, 78
- Moffett, D. A., & Hankins, T. H. 1996, *ApJ*, 468, 779
- Petrova, S. A. 2004, *AAP*, 424, 227
- . 2006, *MNRAS*, 366, 1539
- Popov, M. V., Soglasnov, V. A., Kondrat'Ev, V. I., Kostyuk, S. V., Ilyasov, Y. P., & Oreshko, V. V. 2006, *Astronomy Reports*, 50, 55
- Popov, M. V., & Stappers, B. 2003, *Astronomy Reports*, 47, 660
- Shearer, A., Stappers, B., O'Connor, P., Golden, A., Strom, R., Redfern, M., & Ryan, O. 2003, *Science*, 301, 493
- Sincell, M. W., & Krolik, J. H. 1992, *ApJ*, 395, 553
- Spitkovsky, A. 2006, *ApJ Lett.*, 648, L51
- Staelin, D. H., & Reifenshtein, E. C. 1968, *Science*, 162, 1481
- Weatherall, J. C. 2001, *ApJ*, 559, 196

A Other excitation mechanisms

In this appendix we discuss other excitation mechanisms and point out why they cannot be responsible for Crab GPs, at least for those GPs that show a narrowband structure. In doing so, we assume that the observed band structure is due to emission processes, not propagation.

At $\omega \ll \omega_B$ there are three modes: Alfvén, X and L-O, which can be excited at Cherenkov (except X mode), cyclotron and anomalous cyclotron resonances. We have discussed excitation of the X and the L-O modes at anomalous cyclotron resonances; let us now discuss other possibilities.

A.1 Normal cyclotron resonance

For instability to operate on normal cyclotron resonance particle distribution should be of the loss-cone type. Such distributions may be expected in the outer gap models, which produce secondary particles with non-zero transverse momenta. Effects of magnetic bottling on a down-ward propagating particles will create a loss-cone. In addition, since an outer gap operates near the last closed field lines, it is expected that some particles will drift from open to closed lines. This possibility is attractive since the closed field lines may store particles bouncing between the poles for a long time. Development of the loss-cone instability would then convert this stored energy into radiation. This would create radio emission from closed field lines. Both the X and the L-O modes can be emitted at cyclotron resonance, but the main problem is that emitted frequencies are typically close to cyclotron frequency ω_B , which is some three orders of magnitude higher than observed. In principle, the resonant frequency can be smaller than ω_B as, *e.g.*, in case of backward wave oscillators, but this would require fine tuning the frequencies in one part in a thousand. In addition, inter-band frequency spacing is large, $\sim \omega_B$.

A.2 Alfvén mode

Excitation of Alfvén waves in pulsars has been considered by Lyutikov (2000).

Alfvén waves exist for $0 < \omega < \left(\frac{1}{2} \left(\omega_B^2 + 2\omega_p^2 - \sqrt{(\omega_B^2 + 2\omega_p^2)^2 - 8\omega_B^2\omega_p^2 \cos^2 \theta} \right) \right)^{1/2} \approx \sqrt{2}\omega_p \cos \theta$. At low frequencies, $\omega \ll \omega_p \cos \theta$, $\omega_p \ll \omega_B$, dispersion relation becomes

$$\omega = kc \cos \theta \left(1 - \frac{\omega_p^2}{\omega_B^2} - \frac{(kc)^2 \sin^2 \theta}{\omega_p^2} \right), \text{ for } \omega \ll \omega_p \cos \theta, \omega_p \ll \omega_B \quad (11)$$

Alfvén waves can be excited at Cherenkov resonance at

$$k_{res} c = \frac{\sqrt{2}\omega_p}{\sin \theta} \sqrt{\frac{1}{\gamma_b^2} - \frac{2\omega_p^2}{\omega_B^2}} \quad (12)$$

which requires $\omega_B/(\sqrt{2}\omega_p\gamma_b) > 1$. The resonant frequency is

$$\omega \approx \frac{\sqrt{2}\omega_p}{\gamma_b} \cot \theta, \quad (13)$$

so that at a given angle emission is generated with given ω . Though the resonance condition can, in general, be satisfied, it not clear how to produce different emission bands.

Alfvén waves can also be emitted at anomalous Doppler resonance. For small angles, $\theta \ll \frac{\omega_p^2}{\omega_B k c}$, the resonant frequencies are similar to those of X mode, while for $\theta \gg \frac{\omega_p^2}{\omega_B k c}$ we find

$$k_{res}c = \left(\frac{s\omega_B\omega_p^2}{\gamma_b \cos \theta \sin^2 \theta} \right)^{1/3} \quad (14)$$

In addition, condition $\omega \leq \omega_p$ requires

$$\theta \geq \sqrt{\frac{\omega_B}{\gamma_b\omega_p}} \quad (15)$$

An appealing property of the resonant condition(14) is that it produces a set of frequency bands, separated by frequencies much smaller than cyclotron frequency ω_B . On the other hand, inter-band separation **decreases** with frequency, see Fig 5, contrary to observations. This invalidates the model of Istomin (2004), at least in application to IGPs. In addition, Alfvén waves cannot escape from plasma and need to be converted into escaping modes before they are damped on plasma particles.

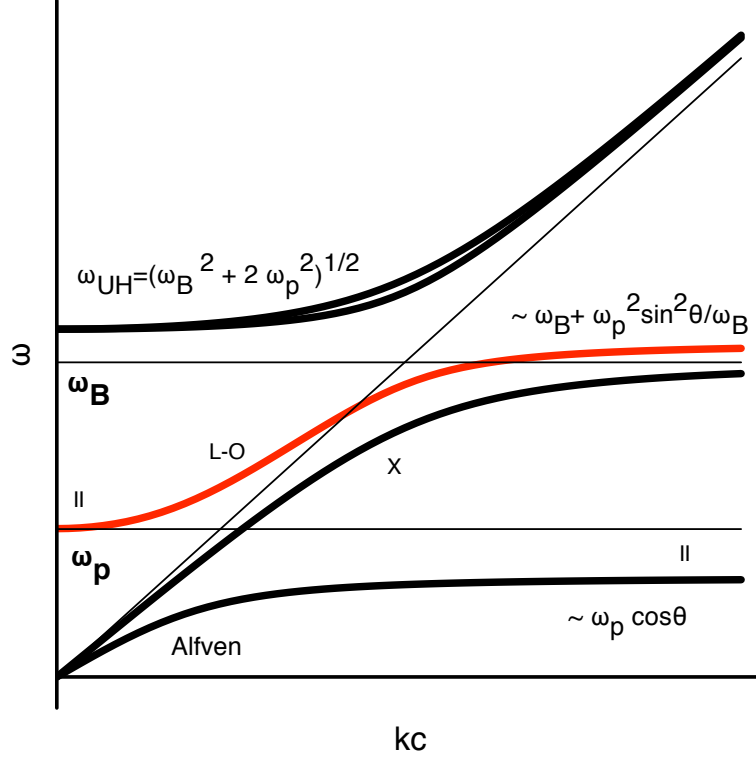


Figure 2: Wave dispersions $\omega(k)$ in pair plasma in strong magnetic field, $\omega_B \gg \omega_p$, for oblique propagation. At low frequencies $\omega \ll \omega_B$ there are three modes labeled X (polarized orthogonally to $\mathbf{k} - \mathbf{B}$ plane), Alfvén and L-O (both polarized in the $\mathbf{k} - \mathbf{B}$ plane). The L-O mode has a resonance at $\sim \omega_B + \omega_p^2 \sin^2 \theta / \omega_B$ and cut-off at $\sqrt{2}\omega_p$. The Alfvén mode has a resonance at $\sim \sqrt{2}\omega_p \cos \theta$. The sign \parallel indicates locations where corresponding waves are nearly longitudinally polarized. The two high frequency, $\omega > \omega_B$, waves with nearly identical dispersion have a cut-off at the upper hybrid frequency $\omega_{UH} = \sqrt{\omega_B^2 + 2\omega_p^2}$.

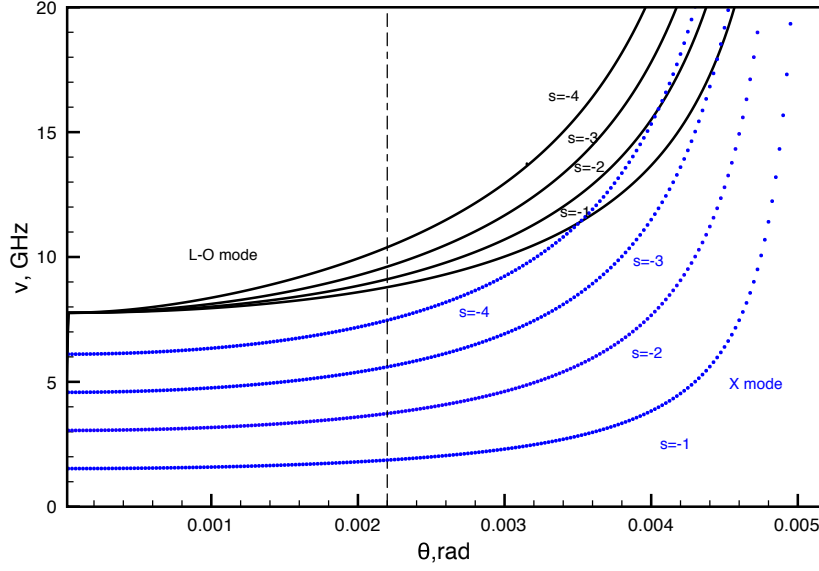


Figure 3: Resonant frequencies for the L-O (solid line) and the X modes (dotted line) for anomalous cyclotron resonance as function of angle between the line of sight and magnetic field for first four resonances $s = -1, \dots -4$. The cut-off of the L-O mode at $\theta = 0$ is at total plasma frequency $\sqrt{2}\omega_p/(2\pi) = 7.76$ GHz. The X modes bands are equally spaced at $\theta = 0$ with $\delta\nu = \frac{\omega_B^3}{\gamma\omega_p^2}$ (corresponding to 1.52 GHz); higher order resonances are not shown. The vertical dashed line gives the best fit values of $\theta = 0.0022$ for resonances on L-O mode.

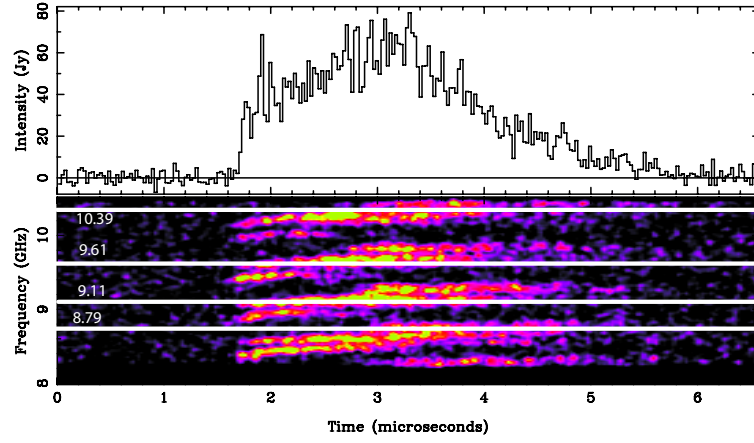


Figure 4: Location of emission bands (white stripes) for the fiducial model. The fitted observations correspond to Fig. 4 of Eilek & Hankins (2007).

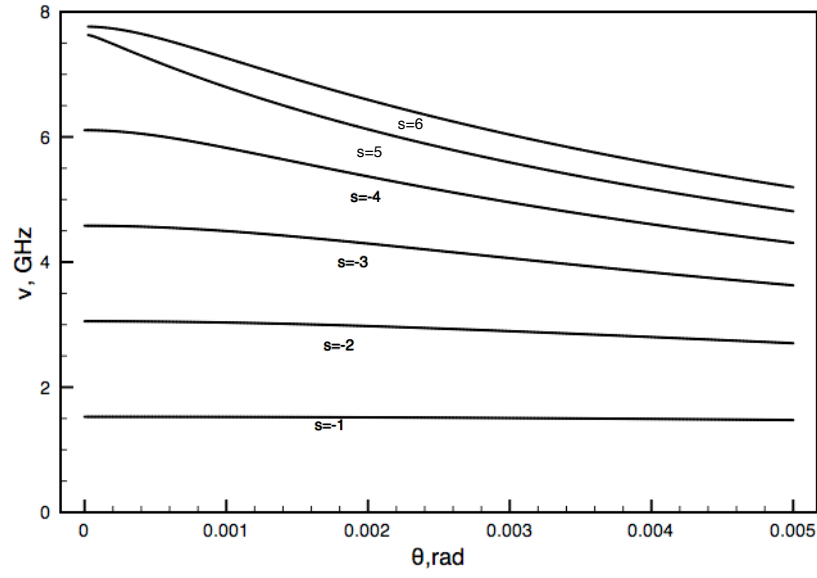


Figure 5: Resonant frequencies for anomalous excitation of Alfvén waves. Parameters are the same as in Fig. 4. Alfvén waves frequencies are limited to $\omega < \sqrt{2}\omega_p \cos \theta$. Contrary to observations, the inter-band spacing decreases with frequency.